Available online at www.sciencedirect.com

SCIENCE DIRECT

Virology 327 (2004) 175–185

VIROLOGY

www.elsevier.com/locate/yviro

Analysis of the interaction between respiratory syncytial virus and lipid-rafts in Hep2 cells during infection

Gaie Brown[a], Chris E. Jeffree[b], Terence McDonald[a], Helen W. McL. Rixon[a], James D. Aitken[c], Richard J. Sugrue[a,*]

[a]*MRC Virology Unit, Institute of Virology, Glasgow G11 5JR, UK*
[b]*Institute of Cell and Molecular Biology, Biological Sciences EM Facility, University of Edinburgh, Edinburgh EH9 3JN, UK*
[c]*IBLS Division of Virology, University of Glasgow, Institute of Virology, Glasgow G11 5JR, UK*

Received 26 February 2004; accepted 4 June 2004
Available online 12 August 2004

Abstract

The assembly of respiratory syncytial virus (RSV) in lipid-rafts was examined in Hep2 cells. Confocal and electron microscopy showed that during RSV assembly, the cellular distribution of the complement regulatory proteins, decay accelerating factor (CD55) and CD59, changes and high levels of these cellular proteins are incorporated into mature virus filaments. The detergent-solubility properties of CD55, CD59, and the RSV fusion (F) protein were found to be consistent with each protein being located predominantly within lipid-raft structures. The levels of these proteins in cell-released virus were examined by immunoelectronmicroscopy and found to account for between 5% and 15% of the virus attachment (G) glycoprotein levels. Collectively, our findings suggest that an intimate association exists between RSV and lipid-raft membranes and that significant levels of these host-derived raft proteins, such as those regulating complement activation, are subsequently incorporated into the envelope of mature virus particles.

Keywords: Respiratory syncytial virus; Virus assembly; Lipid-raft; CD55; CD59; Complement cascade

Introduction

Respiratory syncytial virus (RSV) is the major cause of severe lower respiratory tract disease in several high-risk groups which include young children, the elderly, and immunocompromised adults. The mature and infectious RSV particle comprises a ribonucleoprotein (RNP) core that is surrounded by a viral envelope in which three different glycoproteins, the attachment (G), fusion (F), and small hydrophobic (SH) proteins, are located. Although the structural organization of the mature RSV particle is well characterized (Arslanagic et al., 1996; Bachi and Howe, 1973; Brown et al., 2002a; Norrby et al., 1970; Parry et al., 1979; Roberts et al., 1995), the cellular processes that lead to assembly of the mature virus are still poorly understood. Several host-cell factors have been implicated in the assembly process (Brown et al., 2002a, 2002b; Burke et al., 1998; Ulloa et al., 1998) and furthermore, the involvement of lipid-raft microdomains in the assembly of RSV, as well as in several other paramyxoviruses, has been demonstrated (Ali and Nayak, 2000; Brown et al., 2002b; Henderson et al., 2002; Jeffree et al., 2003; Manie et al., 2000; McCurdy and Graham, 2003; Vincent et al., 2000). It is clear, therefore, that an interaction occurs between the virus and specific host-cell factors during the assembly process.

We have shown previously that in Vero cells, RSV assembly occurs in regions of the cell membrane which are characterized by the presence of caveolin and the sphingolipid, GM1 (Brown et al., 2002a, 2002b; Jeffree et al.,

* Corresponding author. MRC Virology Unit, Institute of Virology, Church Street, Glasgow G11 5JR, UK. Fax: +44 141337 2236.
E-mail address: r.sugrue@vir.gla.ac.uk (R.J. Sugrue).

0042-6822/$ - see front matter © 2004 Elsevier Inc. All rights reserved.
doi:10.1016/j.virol.2004.06.038

2003). These components are associated with specialized lipid-raft structures that have caveolae-like properties (Anderson, 1998; Fra et al., 1995; Kurzchalia et al., 1992; Parton, 1994; Rothberg et al., 1992). Although several enzyme activities are known to reside within caveolae (Razani et al., 2002), recent evidence has suggested that GPI-anchored proteins, such as CD55, are not normally present within caveolae but are enriched within other non-caveolae-like lipid-raft structures (Brown and London, 2000; Friedrichson and Kurzchalia, 1998; Fujimoto, 1996; Mayor et al., 1994; Schnitzer et al., 1995). The complement cascade is an important process in the host's defence against viral infection; however, this process must be controlled to prevent damage to the host and in this respect, CD55 functions by negatively regulating the complement cascade. The work presented here shows that RSV associates with lipid-raft membranes containing CD55 and CD59 and these negative regulators of the complement pathway are incorporated into the envelope of mature RSV particles. This is the first report to demonstrate the assimilation, into the envelope of mature RSV particles, of host-factors that have the potential to regulate the host response to viral infection.

Results and discussion

RSV assembles at regions on the surface of Hep2 cells which are enriched in the complement regulatory proteins CD55 and CD59

CD55 was detected using the polyclonal antibody CD55P and CD59 was detected using both a polyclonal, CD59P, or on occasions a monoclonal antibody, CD59M. The specificity of the polyclonal antibodies in Hep2 cells was confirmed by Western blotting (Figs. 1A and B). Mock-infected refers to the exposure of cells to a mock-inoculum (see Materials and methods). In mock- and virus-infected Hep2 cells, no significant difference was observed in either the CD55 or CD59 protein profile. CD55 migrated as a single 75kDa protein species (CD55/75 k), while CD59 migrated as three closely spaced protein species between 16 and 18kDa. Identical results were obtained using either CD59P or CD59M (data not shown). In contrast, a similar analysis in Vero cells (Fig. 1C) revealed a size difference in CD55 between mock- and virus-infected cells, the significance of which is discussed below.

Confocal microscopy was used to examine the distribution of CD55 and CD59 on the surface of mock- and virus-infected Hep2 cells (Figs. 2A and B). In mock-infected cells double-labeled with CD55P and CD59M, both proteins showed a strong co-localization. In addition, a staining pattern was observed that was slightly filamentous in appearance (Fig. 2A). In virus-infected cells, it was noted that CD55 and CD59 showed a much more pronounced filamentous staining pattern (Fig. 2B, highlighted by white arrows), which was similar to that expected for mature RSV filaments, and both proteins co-localized within these filamentous structures. The distribution of CD55 and CD59 within mature RSV filaments in infected cells was examined in cells which were double-labeled with MAb19, an antibody which recognizes the F protein (Taylor et al., 1992), and either CD55P (Fig. 2C) or CD59P (Fig. 2D), respectively. The appearance of mature filaments stained with MAb19 was clearly visible and furthermore, this analysis showed a high degree of co-localization between the F protein and both CD55 and CD59 within these virus structures (yellow staining pattern in the merged image). The presence of CD55 within the filaments is most clearly visualized in an image taken from a Z-stack gallery of images in which a single cell, double-labeled with CD55P and MAb19, is viewed in the *Y* axis , that is, in cross-section (Fig. 2E). In this image, both the outline of the cell surface and the RSV filaments are visible and the presence of CD55 within the filaments can be seen (indicated by yellow staining).

Although confocal microscopy showed the presence of CD55 and CD59 within virus filaments in Hep2 cells, no increase in the levels of these proteins in virus-infected cells had been observed when analyzed by Western blotting (Figs. 1A and B). This suggests that although virus infection does not alter expression levels of these proteins, their distribution changes in a manner similar to that previously reported for caveolin-1 in Vero cells (Brown et al., 2002a). This change in distribution is a consequence of RSV assembly and the subsequent incorporation of these proteins into the virus envelope.

A more detailed analysis of the surface of virus-infected cells can be achieved using field emission scanning electron microscopy (FE SEM). This technique allows visualization of the mature virus filaments and the distribution of specific antigens on the cell surface. FE SEM has recently been used to analyze the distribution of the G protein in the envelope of mature RSV filaments (Jeffree et al., 2003). The microscope used contains both a secondary electron (SE) detector, which allows surface morphology to be visualized, and a backscatter electron (BSE) detector, which allows the distribution of immunological markers, such as colloidal gold, to be visualized. In this report, FE SEM was used to analyze the distribution of the CD55 protein in mock- and RSV-infected cells (Figs. 3A–E).

Analysis of the surface of mock- and virus-infected cells by SEM at low magnification (Figs. 3A and B) shows morphological changes which occur during virus infection. Microvilli-like projections are present on the surface of Hep2 cells in the absence of virus. However, following infection, many filamentous projections can be seen, which are morphologically similar to the RSV filaments previously observed (Jeffree et al., 2003; Parry et al., 1979; Roberts et al., 1995). Microvilli, which are characterized by the presence of the protein ezrin (Berryman et al., 1995; Bretscher, 1983) were visualized by confocal microscopy using mock- and virus-infected cells that had been stained with an ezrin antibody (Figs. 4A and B). In mock-infected

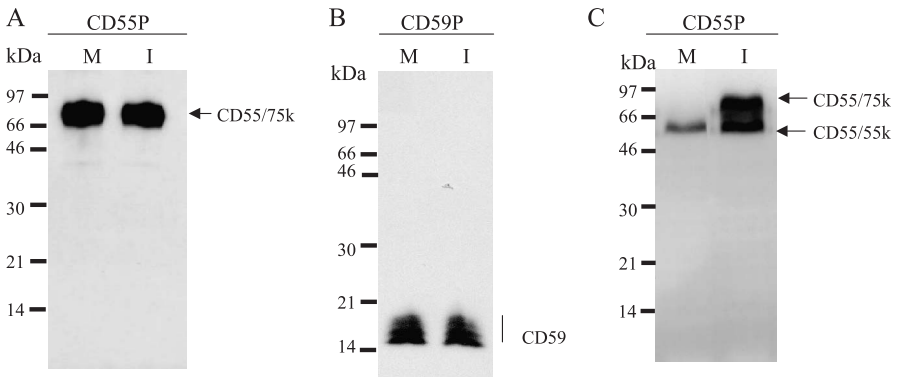

Fig. 1. Specificity of CD55P and CD59P in mock- (M) and RSV-infected (I) cells. Hep2 cells were incubated for 20 h at 33 °C and examined by Western blot analysis using (A) CD55P or (B) CD59P. (C) Vero cells were examined by Western blot analysis using CD55P. The respective protein bands are indicated as are the positions of the molecular mass markers.

cells, an ezrin staining pattern was visible that was clearly filamentous in nature and which was consistent with the microvilli visualized by FE SEM. In contrast, although we were able to visualize ezrin labeling on virus-infected cells, the filamentous projections appeared to be smaller. A similar labeling pattern was observed when mock-and virus-infected cells were stained using phalloidin-FITC which allows staining of the F-actin bundles, a major structural component of microvilli (data not shown). Analysis of virus-infected cells following labeling with an F protein polyclonal antibody (anti-F) and anti-ezrin (Fig. 4C) reveals a distinct staining pattern in each case and that no co-localization of these antigens occurs, demonstrating that the virus filaments and the microvilli are separate structures. Collectively, these

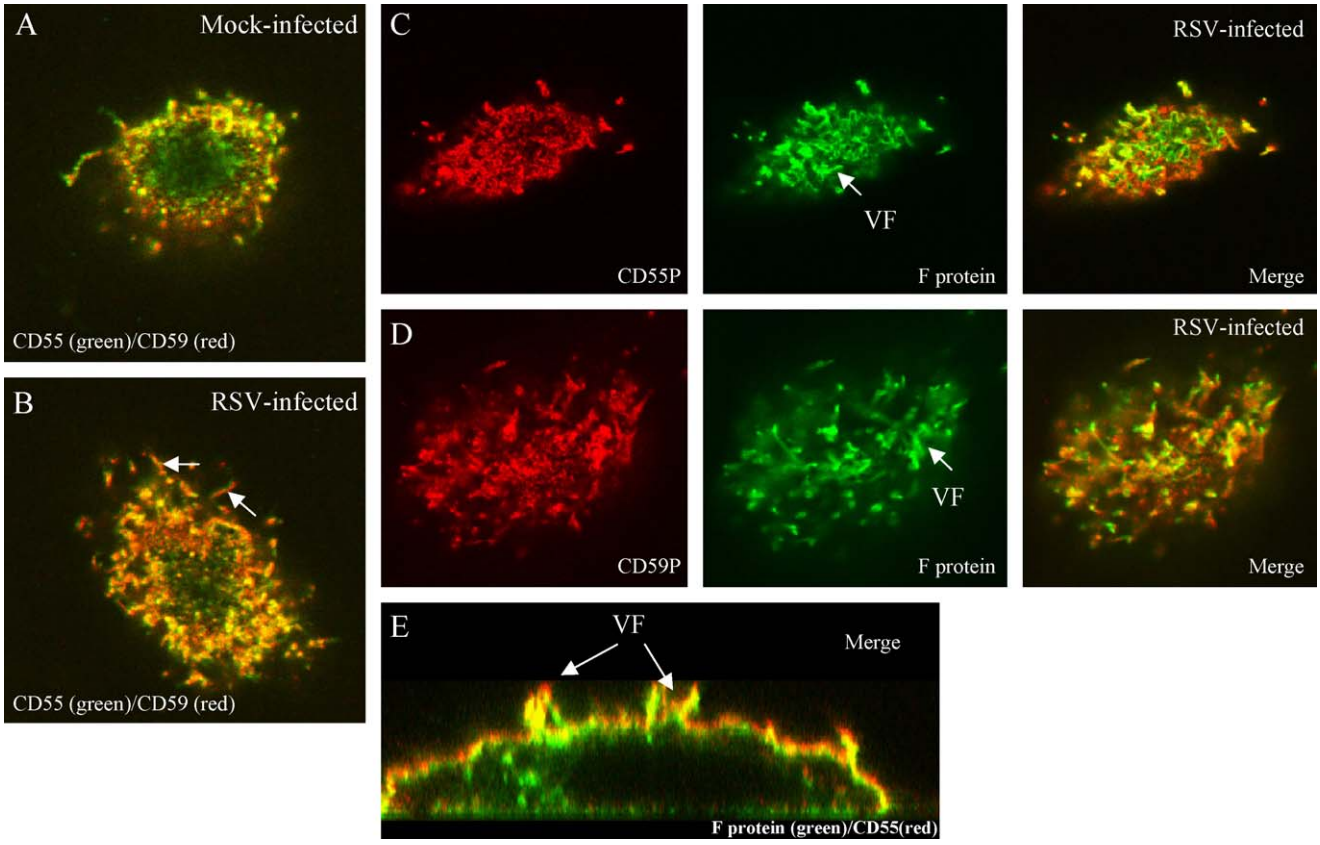

Fig. 2. RSV assembly in Hep2 cells occurs within microdomains that are enriched in CD55 and CD59. Mock- and RSV-infected Hep2 cells were incubated for 20 h at 33 °C and examined by confocal microscopy as described in Materials and methods. Cellular distribution of CD55 (green) and CD59 (red) in (A) mock- and (B) RSV-infected cells. Only the merged images are shown. CD55 and CD59 are present within RSV filaments. RSV-infected cells were labeled with MAb19 (F protein, green) and (C) CD55P (CD55, red) or (D) CD59P (CD59, red) and examined by fluorescence microscopy. (E) A cross-section through a virus-infected cell labeled with MAb19 and CD55P. In all cases, the virus filaments are indicated (VF) by white arrows and co-localization of antigens is indicated by the yellow staining pattern in the merged image.

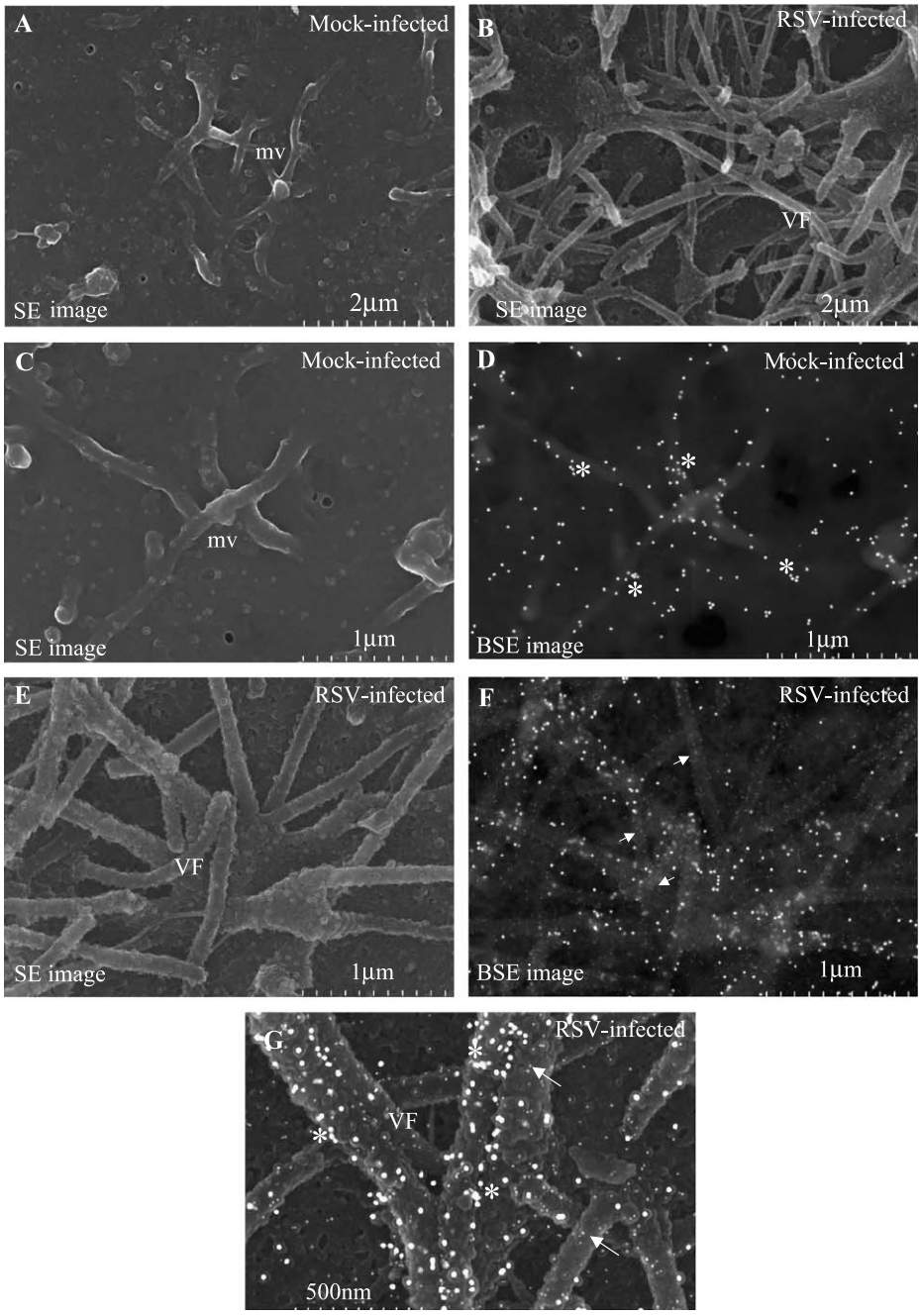

Fig. 3. Distribution of CD55 and the G protein within the envelope of RSV filaments. Mock- and RSV-infected cells were processed for FE SEM as described in Materials and methods. The cells were labeled with CD55P and MAb30 and the presence of bound antibody detected using secondary antibody conjugated to 20 and 5 nm colloidal gold particles, respectively. The individual images obtained using the secondary electron (SE) and backscatter electron (BSE) detectors are shown. Comparison of the surface of (A) mock- and (B) RSV-infected cells at low magnification (magnification ×20,000). Distribution of CD55 and G protein on the surface of mock- (C and D) and virus-infected (E and F) cells (magnification ×40,000). (G) High magnification image showing infected cells in which the SE and BSE images are merged into single images (magnification ×100,000). The 20 nm and 5 nm colloidal gold particles are visualized as large and small white spots, respectively. (*) highlights CD55 protein clusters both in the virus filaments (VF) and the microvilli (mv). The presence of the G protein is highlighted by white arrows.

results suggest that during virus egress, morphological changes occur on the cell surface which are manifested by subtle changes in the structure of microvilli. In this regard, it is interesting to note that changes in the structure of the cytoskeleton have been reported during RSV infection (Bitko et al., 2003; Burke et al., 1998).

Mock- and virus-infected cells were labeled both with MAb30, a reagent that recognizes the virus envelope G protein (Taylor et al., 1992), and CD55P, and the presence of each bound antibody detected using secondary antibodies conjugated to 5 and 20 nm gold, respectively. Analysis of the cell surface by FE SEM at higher magnification allowed the

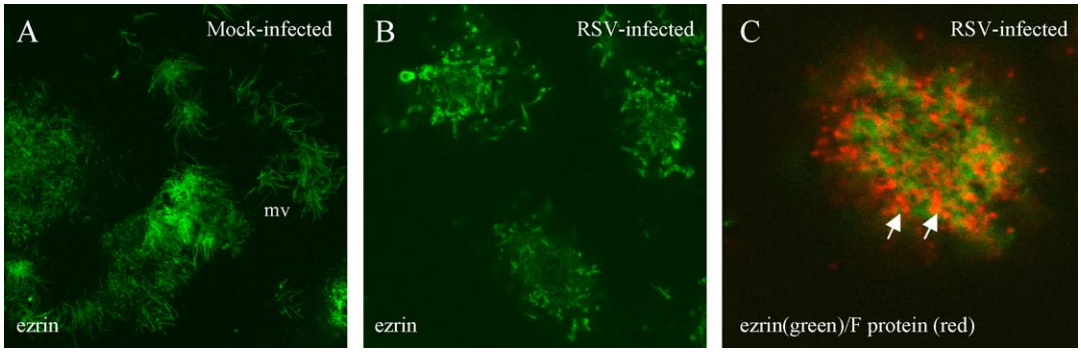

Fig. 4. Morphological changes occur on the cell surface during virus infection. Mock (A) and virus-infected (B) cells were labeled with anti-ezrin and the cells viewed by confocal microscopy. (C) Virus-infected cells labeled with anti-F (red) and anti-ezrin (green) and the distribution of each antigen visualized by confocal microscopy. Only the merged image is shown. The virus filaments (white arrow) and microvilli (mv) are indicated.

labeling pattern of CD55 in mock- and virus-infected cells to be compared (Figs. 3C–F). The presence of the microvilli-like projections on the surface of mock-infected cells was observed (Fig. 3C) and although CD55 was distributed over the whole cell surface, an enrichment of the label was visible on these cellular structures (Fig. 3D, indicated by 20 nm gold particles). Additionally, in many cases, small clusters of gold particles, between 3 and 5 particles, were visualized (Fig. 3D, highlighted by *). Each particle in the 20 nm gold conjugate is coated with approximately 50 molecules of IgG and thus, in theory, can bind the same number of primary antibody molecules (British Biocell International, personal communication). This suggests therefore, that these gold clusters may denote the presence of localized concentrations of CD55 on the cell membrane. As expected, no 5 nm gold particles were detected, indicating the absence of bound MAb30. In contrast, in infected cells, an abundance of virus filaments was visible on the cell-surface (Fig. 3E), which showed strong labeling with both the 5 and 20 nm gold particles (Fig. 3F). This agrees with the fluorescence microscopy observations and confirms the presence of both proteins within the filaments. In some instances, the 20-nm gold particles appeared to form in small clusters suggesting that localized concentrations of CD55 may be present within the virus filaments. This can be seen more clearly in a higher magnification where the images from the SE and BSE detectors are superimposed in a single merged image (Fig. 3G, highlighted by *).

RSV assembly occurs in lipid-rafts containing CD55 and CD59

Lipid-raft membranes were examined in Hep2 cells to determine the extent to which CD55 and CD59 are in these structures. Proteins associated with lipid-raft membranes are soluble in detergents such as NP40 and octyl-β-glucoside but they are characterized by their resistance to solubilization by Triton X-100 at 4 °C (Brown and London, 1998). The Triton-solubility of the F protein, CD55 and CD59 in RSV-infected Hep2 cells was examined by flotation gradient analysis (Fig. 5A).

Total membranes prepared from virus-infected cells were extracted with 1% Triton X-100 and fractionated in a sucrose step-gradient (35% and 5% sucrose) as described in Materials and methods. The presence of the F protein was detected using MAb169 (Rixon et al., 2004) and specific raft proteins in gradient fractions were detected by Western blot analysis using relevant antibodies. In the flotation gradient, although a proportion of the F protein was in the soluble fraction (Fig. 5A, fraction 11), significant levels of the F protein and both the CD55 and CD59 proteins were found in the lipid-raft membrane fraction (Fig. 5A, fraction 3). Furthermore, this fraction also contained caveolin-1 (cav-1) and flotillin-1 (flot-1) (Fig. 5B), two proteins known to associate with lipid-raft membrane structures (Bickel et al., 1997; Sargiacomo et al., 1993). In a similar analysis, transferrin receptor (tfr), a non-raft marker, was found almost exclusively in the non-raft fraction of the gradient. In contrast, flotation gradient analysis of membranes extracted with 1%NP40/60 mM octyl-β-glucoside under identical conditions showed the F protein to be located entirely within the soluble fraction (Fig. 5A) indicating its efficient solubilization by this detergent combination. Thus the data from microscopy and flotation gradient analyses indicate that in Hep2 cells, lipid-raft microdomains containing CD55 and CD59 are primary sites for RSV assembly.

CD55 is present within the envelope of infectious RSV particles

The above data provided evidence that CD55 and CD59 were associated with the envelope of RSV during virus assembly. We therefore wished to determine if these host-derived proteins were present in the envelope of mature virus particles. Non-cell-associated RSV (i.e., cell-free virus in tissue culture medium) loses its predominantly filamentous morphology, becoming more rounded in appearance (Brown et al., 2002a; Lehmkuhl et al., 1980). Virus particles were double-labeled with CD55P or CD59P and MAb 30 and examined by negative staining (Fig. 6). The presence of host-derived proteins and the G protein was detected using

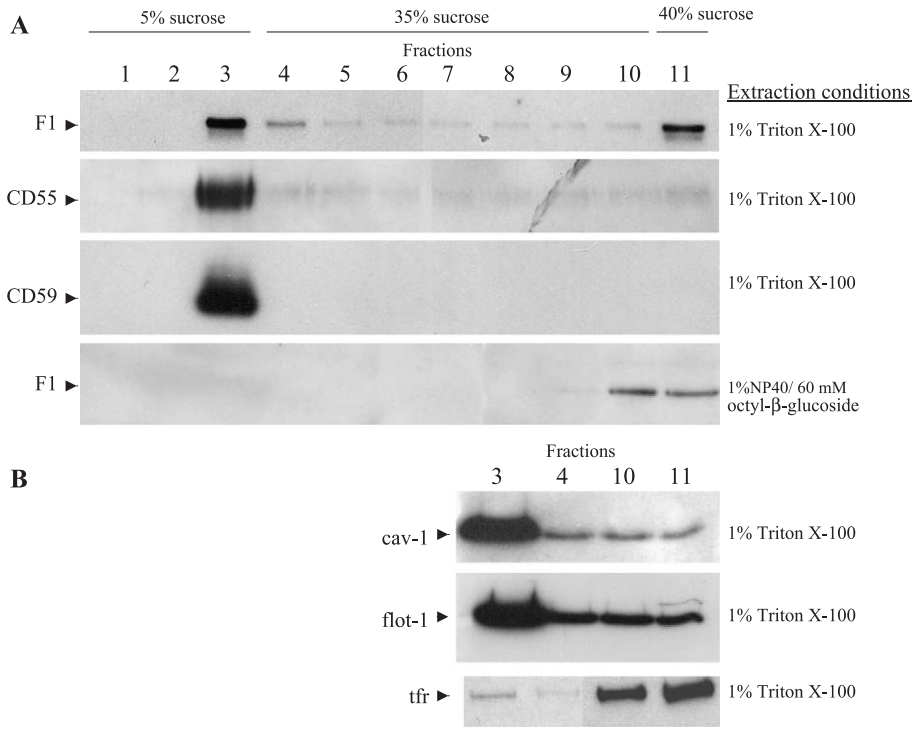

Fig. 5. Flotation gradient analysis of RSV-infected cell membranes. Membranes were prepared from virus-infected cells and examined by flotation gradient analysis as described in Materials and methods. Specific proteins were located in gradient fractions by Western blot analysis using relevant antibodies. (A) Distribution of CD55 and CD59 after Triton-extraction and of the F protein (presence of the F1 subunit) under different extraction conditions. 1 is the top fraction and 11 the bottom fraction. (B) Distribution of the two raft markers, caveolin-1 (cav-1) and flotillin-1 (flot-1) and the non-raft marker transferrin receptor (tfr) are shown.

10 nm and 5 nm gold probe, respectively. As expected, the virus particles were labeled efficiently with MAb 30 over the entire virus particle. In contrast, although labeling of the virus particles with either CD55P or CD59P was observed, the labeling pattern of these antibodies appeared to be concentrated at specific locations in the virus envelope. A comparison of the level of labeling of the G protein with that of either CD55 or CD59 suggested that these host-derived proteins accounted for approximately 5–15% of the detectable gold label on the virus particles.

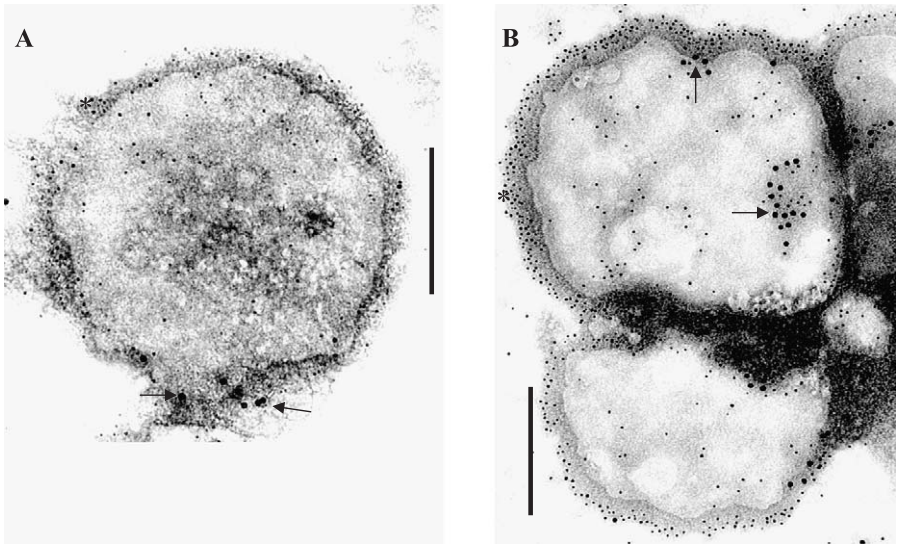

G protein/CD55 G protein/CD59

Fig. 6. Immunonegative staining of virus particles in the inoculum. The virus inoculum was labeled with MAb30 and either (A) CD55P or (B) CD59 and the presence of bound antibody detected using secondary antibody conjugated to 10 nm (CD55 or CD59) and 5 nm (G protein) colloidal gold particles. The labeled samples were then stained as described in Materials and methods (magnification ×40,000). Representative images of labeled virus particles are shown. The presence of 10 nm (→) and 5 nm (*) gold particles are highlighted. Scale bar represents 100 nm.

The above data suggested that these complement regulatory proteins are present in the envelope of virus particles in the inoculum. It was decided therefore to analyze the distribution of CD55 in more detail to determine if it was present in the envelope of mature virus particles during the initial stages of cell attachment. In this study, Vero cells were infected with RSV (prepared in Hep2 cells) and the CD55 analyzed using several methods. In mock-infected cells, a single 55kDa protein species (CD55/55k) was detected by Western blotting which represents the endogenous CD55 expressed in Vero cells (Fig. 1C). This was clearly distinguishable from the 75 kDa CD55 species expressed in Hep2 cells (Fig. 1A), which presumably reflects the cell-specific differences in O-linked glycosylation described previously (e.g., Nakagawa et al., 2001). In virus-infected cells, a level of CD55/55 k similar to that in mock-infected cells was observed, but a second major CD55 species was also present which had a mass similar to the CD55 of Hep2 cells. This was not detected in mock-infected Vero cells suggesting that this second CD55 species represented virus-associated CD55 present in the input virus.

Mock- and RSV-infected Vero cells were examined further by labeling with CD55P and MAb19, and the staining pattern observed using confocal microscopy. In mock-infected cells, CD55P exhibited a diffuse staining pattern throughout the cell (Fig. 7A), suggesting a uniform distribution of CD55. In virus-infected cells labeled with CD55P, the appearance of a more intense punctate staining was observed (Fig. 7A). As expected, staining of infected cells with MAb19 revealed the presence of mature virus filaments, but these virus structures did not co-localize with CD55. Thus, a cell-type specific difference appears to exist in the biochemical characteristics of the raft structures used during virus assembly since CD55 cannot be detected in virus filaments in Vero cells by fluorescence microscopy, whereas it is evident in the virus filaments that form on Hep2 cells.

In contrast, the punctate CD55 staining pattern observed in virus-infected cells appeared to show a strong co-localization with MAb19. We examined the possibility that this alternative staining pattern represented the initial sites of contact between the virus envelope and host-cell membrane following virus attachment, that is, input virus. RSV-infected cells were examined during the initial phase of infection (0–4 h PI) using fluorescence microscopy and FE SEM. This allowed simultaneous visualization of the distribution of both CD55 and virus particles at the early stages of infection. Cells were exposed to the virus for between 0.5 and 4 h after which the cells were extensively

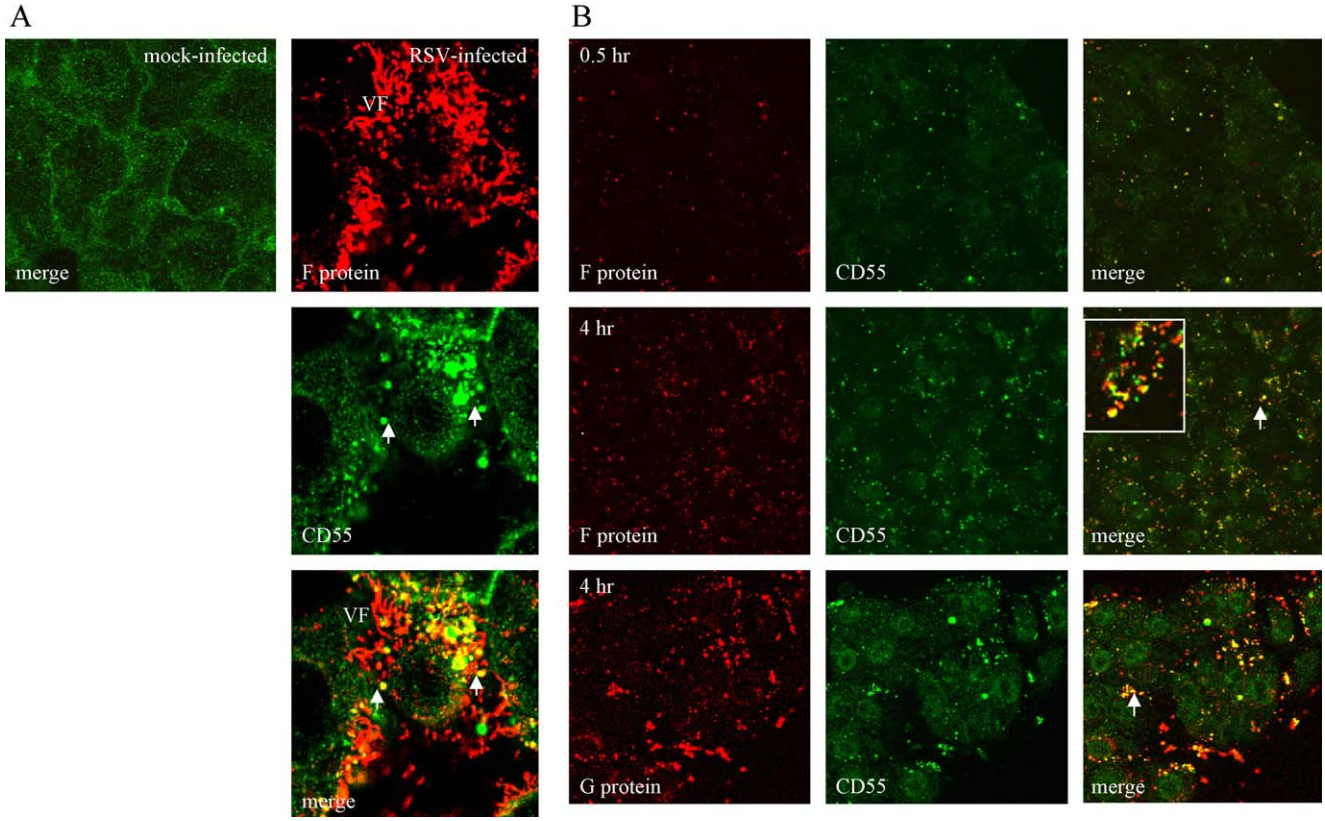

Fig. 7. Distribution of virus antigen and CD55 in RSV-infected Vero cells. (A) Vero cells were mock-infected or infected with RSV and the cellular distribution of CD55 (green) and the F protein (red) examined at 20 h PI by fluorescence microscopy. (B) The cellular distribution of CD55 (green) and the virus antigens (red) was examined by fluorescence microscopy during the initial stages of infection. Cells were exposed to the virus inoculum for either 0.5 or 4 h before processing for fluorescence microscopy. The cells were labeled with MAb19 (F protein) or MAb30 (G protein) and CD55P. Virus filaments are indicated (VF) and in all cases, co-localization of CD55 with the virus antigens is indicated by the yellow staining pattern (highlighted by white arrows).

washed, fixed and double-labeled with CD55P and either MAb19 or MAb30 (Fig. 7B). Analysis by fluorescence microscopy revealed co-localization between CD55 and MAb19 very early in infection, starting within 0.5 h and increasing up to at least 4 h PI, which is consistent with an increase in virus attachment over a 4 h time period.

FE SEM was used to analyze the distribution of CD55, MAb30 and virus particles on the surface of Vero cells, following a brief exposure to the virus inoculum (Fig. 8). The presence of spherical particles was observed on the cell surface which were indistinguishable from the virus particles in the virus inoculum detected by immunonegative TEM. These particles ranged in diameter from 200 to 300 nm and were heavily labeled with MAb30, confirming their viral origin. Vero cells were double-labeled with CD55P and MAb30 and the presence of each antigen was visualized using 20 nm (CD55) and 5 nm (G protein) gold probe, respectively (Fig. 8, inset). At high magnification, the different sizes of gold probe on the cell-surface were clearly distinguishable, allowing determination of the distribution of each antigen. These structures showed a CD55 labeling pattern similar to that observed on virus particles in the virus inoculum. Collectively, the results obtained by light (Fig. 7) and electron microscopy (Figs. 6 and 8) support the conclusion that high levels of these complement regulatory proteins are incorporated into the envelope of mature virus particles and that these proteins are present within the virion during the initial stages of cell attachment.

This report provides that evidence in Hep2 cells, RSV associates with lipid-raft membranes that are enriched in the complement regulatory proteins, CD55 and CD59, high levels of which are subsequently incorporated into the envelope of maturing virus particles. Incorporation of CD55 and CD59 is presumably a consequence of their presence within the lipid-raft structures which are used as platforms for virus assembly (Briggs et al., 2003) and results in the formation of a viral envelope that contains both virus-encoded proteins and an array of host-derived proteins. Although CD55 and CD59 are present within the virus envelope, it is unlikely that they represent specific requirements for virus assembly. We have observed the formation of RSV filaments on the surface of infected CHO cells, a cell line that does not express CD55 (unpublished observations). However, these cell-derived proteins may impart important properties to the virus since, for example, CD55, which is expressed on the surface of many cell types (Miwa and Song, 2001), inhibits the formation of the C3 and C5 convertases and accelerates the degradation of these molecules (Fujita et al., 1987), thus negatively regulating the complement cascade. Viruses have developed different strategies with which to counter the effects of the complement system (reviewed in Favoreel et al., 2003) and one such strategy is the incorporation of cellular complement control factors. For example, CD55 and CD59 have been shown to be incorporated into the envelope of several viruses during virus assembly, including both DNA (e.g., cytomegalovirus, Spear et al., 1995) and RNA viruses (e.g., HIV, Frank et al., 1996; Marschang et al., 1995; Schmitz et al., 1995; Stoiber et al., 1996). However, of the viruses known to incorporate these host factors into mature virus particles, the role of

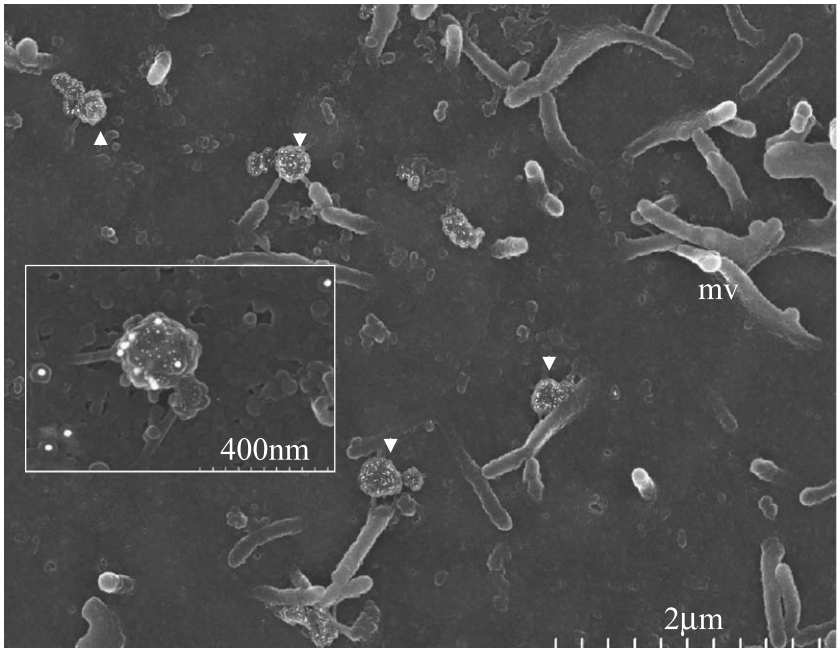

Fig. 8. CD55 is present within the envelope of RSV particles during the initial stages of cell attachment. (A) Cells were exposed to the virus inoculum for 4 h after which they were fixed, labeled with MAb30 and prepared for FE SEM as described in Materials and methods. The presence of microvilli (mv) and bound virus particles (▽) can be seen at low magnification (magnification ×20,000). The presence of bound gold (10 nm) on the virus particles is visible as white spots. Inset, cells were exposed to the virus inoculum for 4 h after which they were fixed and labeled with CD55P and MAb30. The distribution of CD55 (20 nm) and the G protein (5 nm) can be seen at high magnification (magnification ×130,000) in these merged images as large and small white spots, respectively.

CD55 in HIV-1 replication is perhaps the best characterized (Stoiber et al., 1997). In this case, the presence of virus-associated CD55 imparts potentially important biological properties to the mature HIV-1 particles, such as an increased resistance to complement-mediated lysis (Saifuddin et al., 1995, 1997; Stoiber et al., 1996). It is possible that the presence of these proteins within the RSV envelope may protect the virus in a similar manner. For example, RSV is one of several respiratory pathogens that cause the middle ear infection, otitis media, in neonates (Heikkinen, 2001; Heikkinen and Chonmaitree, 2003), a condition that is characterized by a strong complement activation (Narkio-Makela et al., 1999). Thus, the possibility exists that the presence of CD55 in the virus envelope may protect the virus from complement inactivation during infection. However, at present, the biological consequences of the virus-associated complement proteins remain to be established.

Materials and methods

Cells and viruses

The RSV A2 strain was used throughout this study. Hep2 cells were maintained in Dulbecco's Modified Eagle's Medium (DMEM) supplemented with 10% fetal calf serum (FCS) and antibiotics.

Preparation of mock- and RSV inocula

Hep2 cells were either infected with RSV or left uninfected (mock-infected) and incubated at 33 °C for 3 days in DMEM supplemented with 2% FCS before harvesting. The cells, together with tissue culture medium, were collected and clarified by centrifugation (2000 × *g* for 15 min) to remove the cell debris. The presence of RSV in the RSV-inoculum and the removal of cell debris from both the mock- and RSV-inocula was confirmed by TEM.

Antibodies

Antibodies against the RSV F (MAb19) and G (MAb30) proteins were obtained from Geraldine Taylor (IAH, Compton, UK). The F protein antibody, MAb169, was prepared by immunizing mice with bacterially expressed recombinant HRSV A2 F protein and the F protein polyclonal antibody was provided by Jose Melero (Instituto de Salud Carlos III, Madrid, Spain). The CD55 antibody was provided by Ian Goodfellow and David Evans (Virology Division, University of Glasgow, UK) and the CD59 antibodies were obtained from Brad Spiller (University of Cardiff, UK). The caveolin-1 (N20) antibody was purchased from Santa Cruz Biotechnology, the ezrin and flotillin antibodies were purchased from BD Transduction Laboratories and the transferrin receptor antibody was purchased from Zymed Laboratories.

Western blotting

Western blotting was performed as described previously (Brown et al., 2002a). Briefly, proteins were separated by SDS PAGE after which they were transferred by Western blotting on to PVDF membranes. The membranes were washed, blocked with 1% Marvel, and probed with specific primary antibodies for 1 h. The membranes were then washed, probed either with goat anti-mouse or anti-rabbit IgG (whole molecule) peroxidase conjugate (Sigma) as appropriate and the protein bands visualized using the ECL protein detection system (Amersham). Apparent molecular masses were estimated using Rainbow protein markers (Amersham) in the molecular weight range 14.3–220 kDa.

Immunofluorescence

Cells were seeded on 13 mm glass coverslips and either mock- or RSV-infected and incubated overnight at 33 °C after which the cells were fixed with 3% paraformaldehyde in PBS for 30 min at 4 °C. The fixative was removed and the cells washed 5 times with PBS + 1 mM glycine and once with PBS. The fixed cells were permeabilized with 0.1% saponin/PBS at 25 °C for 15 min. Following incubation at 25 °C for 1 h with the primary antibody, the cells were washed and incubated for a further 1 h with the secondary antibody, either goat anti-mouse or anti-rabbit IgG (whole molecule) conjugated to either Cy5 or FITC as appropriate (1/100 dilution). The stained cells were mounted on slides using Citifluor and visualized with a Zeiss Axioplan 2 confocal microscope. The images were processed using LSM 510 v2.01 software.

Field emission scanning electron microscopy (FE SEM)

This was performed as described previously (Jeffree et al., 2003). Cells on glass coverslips were either mock-infected or infected with RSV and incubated overnight at 33 °C. Cells were fixed with 0.5% glutaraldehyde in PBS at 4 °C for 30 min. The fixed monolayers were incubated in PBS supplemented with 2 mM glycine for 20 min and then washed extensively with PBS. The cells were incubated at 25 °C for 4 h with MAb30 and CD55P, washed, and then incubated for a further 4 h either in goat anti-mouse IgG (whole molecule) conjugated to 5 nm colloidal gold (Sigma) or goat anti-rabbit IgG (whole molecule) conjugated to 20 nm colloidal gold (British Biocell International). The monolayers were washed with PBS, fixed with 2.5% glutaraldehyde in PBS and processed for SEM as described previously. The samples were visualized in a Hitachi 4700 F field emission scanning electron microscope using appropriate settings and digital images were recorded using Hitachi FE PCSEM (ver 3.2) software.

Immunonegative staining

A droplet of the clarified tissue culture medium from infected cells was placed on a formvar-coated grid and the virus adsorbed for 10 min. Grids were inverted on to a droplet of primary antibody for 3 h, washed in PBS, and then incubated for a further 1.5 h with anti-rabbit IgG (whole molecule) 10 nm colloidal gold and anti-mouse IgG (whole molecule) 5 nm colloidal gold conjugates (British Biocell International). The grids were then washed, stained with uranyl acetate (saturated in 50:50 ethanol/water) and counter-stained with lead citrate. Samples were examined using a Jeol 100S transmission electron microscope.

Acknowledgment

We thank Duncan McGeoch for critical review of the manuscript.

References

Ali, A., Nayak, D.P., 2000. Assembly of Sendai virus: M protein interacts with F and HN proteins and with the cytoplasmic tail and transmembrane domain of F protein. Virology 276, 289–303.

Anderson, R.G.W., 1998. The caveolae membrane system. Annu. Rev. Biochem. 67, 199–225.

Arslanagic, E., Matsumoto, M., Suzuki, K., Nerome, K., Tsutsumi, H., Hung, T., 1996. Maturation of respiratory syncytial virus within HEp-2 cell cytoplasm. Acta Virol. 40, 209–214.

Bachi, T., Howe, C., 1973. Morphogenesis and ultrastructure of respiratory syncytial virus. J. Virol. 12, 1173–1180.

Berryman, M., Gary, R., Bretscher, A., 1995. Ezrin oligomers are major cytoskeletal components of placental microvilli: a proposal for their involvement in cortical morphogenesis. J. Cell Biol. 131, 1231–1242.

Bickel, P.E., Scherer, P.E., Schnitzer, J.E., Oh, P., Lisanti, M.P., Lodish, H.F., 1997. Flotillin and epidermal surface antigen define a new family of caveolae-associated integral membrane proteins. J. Biol. Chem. 272, 13793–13802.

Bitko, V., Oldenburg, A., Garmon, N.E., Barik, S., 2003. Profilin is required for viral morphogenesis, syncytium formation, and cell-specific stress fiber induction by respiratory syncytial virus. BMC Microbiol. 3, 9 (Electronic publication).

Bretscher, A., 1983. Purification of an 80,000-dalton protein that is a component of the isolated microvillus cytoskeleton, and its localization in nonmuscle cells. J. Cell Biol. 97, 425–432.

Briggs, J.A., Wilk, T., Fuller, S.D., 2003. Do lipid rafts mediate virus assembly and pseudotyping? J. Gen. Virol. 84, 757–768.

Brown, D.A., London, E., 1998. Functions of lipid rafts in biological membranes. Annu. Rev. Cell Dev. Biol. 14, 111–136.

Brown, D.A., London, E., 2000. Structure and function of sphingolipid- and cholesterol-rich membrane rafts. J. Biol. Chem. 275, 17221–17224.

Brown, G., Aitken, J., Rixon, H.W.McL., Sugrue, R.J., 2002a. Caveolin-1 is incorporated into mature RSV particles during virus assembly on the surface of virus-infected cells. J. Gen. Virol. 83, 611–621.

Brown, G., Rixon, H.W.McL., Sugrue, R.J., 2002b. Respiratory syncytial virus assembly occurs in GM1-rich regions of the host-cell membrane and alters the cellular distribution of tyrosine phosphorylated caveolin-1. J. Gen. Virol. 83, 1841–1850.

Burke, E., Dupuy, L., Wall, C., Barik, S., 1998. Role of cellular actin in the gene expression and morphogenesis of human respiratory syncytial virus. Virology 252, 137–148.

Favoreel, H.W., Van de Walle, G.R., Nauwynck, H.J., Pensaert, M.B., 2003. Virus complement evasion strategies. J. Gen. Virol. 84, 1–15.

Fra, A.M., Williamson, E., Simons, K., Parton, R.G., 1995. De novo formation of caveolae in lymphocytes by expression of VIP21-caveolin. Proc. Natl. Acad. Sci. U.S.A. 92, 8655–8659.

Frank, I., Stoiber, H., Godar, S., Most, J., Stockinger, H., Katinger, H.W.D., 1996. Acquisition of host cell-surface-derived molecules by HIV-1. AIDS 10, 1611–1620.

Friedrichson, T., Kurzchalia, T.V., 1998. Microdomains of GPI-anchored proteins in living cells revealed by crosslinking. Nature 394, 802–805.

Fujimoto, T., 1996. GPI-anchored proteins, glycosphingolipids, and sphingomyelin are sequestered to caveolae only after crosslinking. J. Histochem. Cytochem. 44, 929–941.

Fujita, T., Inoue, T., Ogawa, K., Iida, K., Tamura, N., 1987. The mechanism of action of decay-accelerating factor (DAF). DAF inhibits the assembly of C3 convertases by dissociating C2a and Bb. J. Exp. Med. 66, 1221–1228.

Heikkinen, T., 2001. The role of respiratory viruses in otitis media. Vaccine 19 (Suppl. l1), S51–S55.

Heikkinen, T., Chonmaitree, T., 2003. Importance of respiratory viruses in acute otitis media. Clin. Microbiol. Rev. 16, 230–241.

Henderson, G., Murray, J., Yeo, R.P., 2002. Sorting of the respiratory syncytial virus matrix protein into detergent-resistant structures is dependent on cell-surface expression of the glycoproteins. Virology 300, 244–254.

Jeffree, C.J., Rixon, H.W.McL., Brown, G., Aitken, J., Sugrue, R.J., 2003. Distribution of the attachment (G) glycoprotein and GM1 within the envelope of mature respiratory syncytial virus filaments revealed using field emission scanning electron microscopy. Virology 306, 254–267.

Kurzchalia, T.V., Dupree, P., Monier, S., 1992. VIP21-Caveolin, a protein of the trans-Golgi network and caveolae. FEBS Lett. 346, 88–91.

Lehmkuhl, H.D., Smith, M.H., Cutlip, R.C., 1980. Morphogenesis and structure of caprine respiratory syncytial virus. Arch. Virol. 65, 269–276.

Manie, S.N., Debreyne, S., Vincent, S., Gerlier, D., 2000. Measles virus structural components are enriched into lipid raft microdomains: a potential cellular location for virus assembly. J. Virol. 74, 305–311.

Marschang, P., Sodroski, J., Wurzner, R., Dierich, M.P., 1995. Decay-accelerating factor (CD55) protects human immunodeficiency virus type 1 from inactivation by human complement. Eur. J. Immunol. 25, 285–290.

Mayor, S., Rothberg, K.G., Maxfield, F.R., 1994. Sequestration of GPI-anchored proteins in caveolae triggered by cross-linking. Science 264, 1948–1951.

McCurdy, L.H., Graham, B.S., 2003. Role of plasma membrane lipid microdomains in respiratory syncytial virus filament formation. J. Virol. 77, 1747–1756.

Miwa, T., Song, W.C., 2001. Membrane complement regulatory proteins: insight from animal studies and relevance to human diseases. Int. Immunopharmacol. 1, 445–459.

Nakagawa, M., Mizuno, M., Kawada, M., Uesu, T., Nasu, J., Takeuchi, K., Okada, H., Endo, Y., Fujitam, Tsuji, T., 2001. J. Gastroen. Hepatol. 16, 184–189.

Narkio-Makela, M., Jero, J., Meri, S., 1999. Complement activation and expression of membrane regulators in the middle ear mucosa in otitis media with effusion. Clin. Exp. Immunol. 116, 401–409.

Norrby, E., Marusyk, H., Orvell, C., 1970. Morphogenesis of respiratory syncytial virus in a green monkey kidney cell line (Vero). J. Virol. 6, 237–242.

Parry, J.E., Shirodaria, P.V., Pringle, C.R., 1979. Pneumoviruses: the cell surface of lytically and persistently infected cells. J. Gen. Virol. 44, 479–491.

Parton, R.G., 1994. Ultrastructural localization of gangliosides; GM1 is concentrated in caveolae. J. Histochem. Cytochem. 42, 155–166.

Razani, B., Woodman, S.E., Lisanti, M.P., 2002. Caveolae: from cell biology to animal physiology. Pharmacol. Rev. 54, 431–467.

Rixon, H.W.McL., Brown, G., Aitken, J., McDonald, T., Graham, S., Sugrue, R.J., 2004. The small hydrophobic (SH) protein accumulates within lipid-raft structures of the Golgi complex during respiratory syncytial virus (RSV) infection. J. Gen. Virol. 85, 1153–1165.

Roberts, S.R., Compans, R.W., Wertz, G.W., 1995. Respiratory syncytial virus matures at the apical surfaces of polarized epithelial cells. J. Virol. 69, 2667–2673.

Rothberg, K.G., Heuser, J.E., Donzell, W.C., Ying, Y.S., Glenney, J.R., Anderson, R.G., 1992. Caveolin, a protein component of caveolae membrane coats. Cell 68, 673–682.

Saifuddin, M., Parker, C.J., Peeples, M.E., Gorny, M.K., Zolla-Pazner, S., Ghassemi, M., Rooney, I.A., Atkinson, J.P., Spear, G.T., 1995. Role of virion-associated glycosylphosphatidylinositol-linked proteins CD55 and CD59 in complement resistance of cell line-derived and primary isolates of HIV-1. J. Exp. Med. 182, 501–509.

Saifuddin, M., Hedayati, T., Atkinson, J.P., Holguin, M.H., Parker, C.J., Spear, G.T., 1997. Human immunodeficiency virus type 1 incorporates both glycosylphosphatidylinositol-anchored CD55 and CD59 and integral membrane CD46 at levels that protect from complement-mediated destruction. J. Gen. Virol. 78, 1907–1911.

Sargiacomo, M., Sudol, M., Tang, Z., Lisanti, M.P., 1993. Signal transducing molecules and glycosyl-phosphatidylinositol-linked proteins form a caveolin-rich insoluble complex in MDCK cells. J. Cell Biol. 122, 789–807.

Schmitz, J., Zimmer, J.P., Kluxen, B., Aries, S., Bogel, M., Gigli, I., Schmitz, H., 1995. Antibody-dependent complement-mediated cytotoxicity in sera from patients with HIV-1 infection is controlled by CD55 and CD59. J. Clin. Invest. 96, 1520–1526.

Schnitzer, J.E., McIntosh, D.P., Dvorak, A.M., Liu, J., Oh, P., 1995. Separation of caveolae from associated microdomains of GPI-anchored proteins. Science 269, 1435–1439.

Spear, G.T., Lurain, N.S., Parker, C.J., Ghassemi, M., Payne, G.H., Saifuddin, M., 1995. Host cell-derived complement control proteins CD55 and CD59 are incorporated into the virions of two unrelated enveloped viruses. Human T cell leukemia/lymphoma virus type I (HTLV-I) and human cytomegalovirus (HCMV). J. Immunol. 155, 4376–4381.

Stoiber, H., Pinter, C., Siccardi, A.G., Clivo, A., Dierich, M.P., 1996. Efficient destruction of human immunodeficiency virus in human serum by inhibiting the protective action of complement factor H and decay accelerating factor (DAF CD55). J. Exp. Med. 183, 307–310.

Stoiber, H., Clivio, A., Dierich, M.P., 1997. Role of complement in HIV infection. Annu. Rev. Immunol. 15, 649–674.

Taylor, G., Stott, E.J., Furze, J., Ford, J., Sopp, P., 1992. Protective epitopes on the fusion protein of respiratory syncytial virus recognized by murine and bovine monoclonal antibodies. J. Gen. Virol. 73, 2217–2223.

Ulloa, L., Serra, R., Asenjo, A., Villanueva, N., 1998. Interactions between cellular actin and human respiratory syncytial virus (HRSV). Virus Res. 53, 13–25.

Vincent, S., Gerlier, D., Manie, S.N., 2000. Measles virus assembly within membrane rafts. J. Virol. 74, 9911–9915.